⌘ *Author's Choice*

THE JOURNAL OF BIOLOGICAL CHEMISTRY VOL. 283, NO. 25, pp. 17721–17730, June 20, 2008
© 2008 by The American Society for Biochemistry and Molecular Biology, Inc. Printed in the U.S.A.

Hydrogen Peroxide Promotes Aβ Production through JNK-dependent Activation of γ-Secretase*[S]

Received for publication, January 2, 2008, and in revised form, April 23, 2008 Published, JBC Papers in Press, April 23, 2008, DOI 10.1074/jbc.M800013200

Chengyong Shen[‡], Yongfeng Chen[‡], Huaqing Liu[‡], Kejing Zhang[‡], Ting Zhang[‡], Anning Lin[§], and Naihe Jing[‡1]

From the [‡]Laboratory of Molecular Cell Biology, Key Laboratory of Stem Cell Biology, Institute of Biochemistry and Cell Biology, Shanghai Institutes for Biological Sciences, Chinese Academy of Sciences, Shanghai 200031, China and the [§]Ben May Department for Cancer Research, the University of Chicago, Chicago, Illinois 60637

Accumulation of senile plaques composed of amyloid β-peptide (Aβ) is a pathological hallmark of Alzheimer disease (AD), and Aβ is generated through the sequential cleavage of amyloid precursor protein (APP) by β- and γ-secretase. Although oxidative stress has been implicated in the AD pathogenesis by inducing Aβ production, the underlying mechanism remains elusive. Here we show that the pro-oxidant H_2O_2 promotes Aβ production through c-Jun N-terminal kinase (JNK)-dependent activation of γ-secretase. Treatment with H_2O_2 induced significant increase in the levels of intracellular and secreted Aβ in human neuroblastoma SH-SY5Y cells. Although γ-secretase-mediated cleavage of APP or C99 was enhanced upon H_2O_2 treatment, expression of APP or its α/β-secretase-mediated cleavage was not affected. Silencing of the stress-activated JNK by small interfering RNA or the specific JNK inhibitor SP600125 reduced H_2O_2-induced γ-secretase-mediated cleavage of APP. JNK activity was augmented in human brain tissues from AD patients and active JNK located surrounding the senile plaques in the brain of AD model mouse. Our data suggest that oxidative stress-activated JNK may contribute to senile plaque expansion through the promotion of γ-secretase-mediated APP cleavage and Aβ production.

Alzheimer disease (AD)[2] is characterized by three neuropathological hallmarks in the brain tissues of patients: senile plaques (SP), neurofibrillary tangles, and neuronal loss. Senile plaques are largely composed of amyloid β-peptide (Aβ), which is considered to be the primary cause of the disease (1). The level of Aβ in the brain is low in young AD subjects, and it starts to increase and accumulate with aging. The increase of Aβ is slow at the beginning but gradually accelerates in an exponential manner, which eventually reaches a catastrophic situation (2, 3).

Proteolytic processing of amyloid precursor protein (APP) in sequence by β- and γ-secretase leads to the formation of Aβ peptide (4). The yield of two main Aβ species ($Aβ_{40}$ and $Aβ_{42}$) is determined by γ-secretase, which is a member of the intramembrane protease superfamily (5). γ-Secretase has an unusual aspartyl protease activity, because it catalyzes the proteolytic events within lipid bilayers (6). Despite enormous progresses made in biochemical characterization of γ-secretase (7–10), relatively few studies have elaborated the regulation of endogenous γ-secretase activity, which is responsible for Aβ generation in the sporadic AD pathogenesis.

Oxidative stress results from an imbalance of aerobic metabolism and imposes a serious threat to cellular homeostasis. Highly reactive oxygen species (ROS) oxidize lipids, proteins, and DNA, leading to tissue damage and cell death (11). Brains of AD patients exhibit abnormally high amounts of ROS in senile plaques and neurofibrillary tangles bearing neurons (12, 13). There is a strong correlation between the intensity of free radical generation and Aβ neurotoxicity. Aβ can trigger the production of ROS and increase H_2O_2 accumulation in a Cu^+/Fe^{2+}-dependent manner, thereby damaging vulnerable neurons (14). The dysfunction and degeneration of synapses in AD may be related to Aβ-induced oxidative stress, because exposure of synapses to Aβ impairs the function of membrane ion channels and glutamate transporters in an oxidative stress-dependent manner (4). Interestingly, oxidative stress has also been reported to enhance Aβ levels and promote Aβ accumulation (15–18). Treatment with anti-oxidant reagents, such as vitamin E, reduces Aβ levels and amyloid plaques in AD model Tg2576 mice (19). Therefore, accumulation of ROS and elevation of Aβ level may exacerbate a vicious cycle in the progressive Aβ accumulation and AD pathogenesis.

The molecular mechanism underlying the promotion of Aβ production by oxidative stress is not completely understood. It has been reported that H_2O_2 can induce APP expression and thereby enhance Aβ production in mammalian lenses (16). Low concentration of H_2O_2 has been shown to potentiate the promoter activity of β-secretase (17) and enhance its expression

* This work was supported, in whole or in part, by National Institutes of Health Grant CA100460 (to A. L.). This work was also supported by National Natural Science Foundation of China Grants 30623003 and 30721065 (to N. J.), National Key Basic Research and Development Program of China Grants 2005CB522704, 2006CB943902, and 2007CB947101 (to N. J.), National 863 Plan Project 2006AA02Z186 (to N. J.), Shanghai Key Project of Basic Science Research Grants 06DJ14001 and 06DZ22032 (to N. J.), and Council of Shanghai Municipal Government for Science and Technology Grant 05814578 (to N. J.). The costs of publication of this article were defrayed in part by the payment of page charges. This article must therefore be hereby marked "*advertisement*" in accordance with 18 U.S.C. Section 1734 solely to indicate this fact.

⌘ *Author's Choice*—Final version full access.

[S] The on-line version of this article (available at http://www.jbc.org) contains supplemental Figs. S1–S3.

[1] To whom correspondence should be addressed. Tel.: 86-21-5492-1381; Fax: 86-21-5492-1011; E-mail: njing@sibs.ac.cn.

[2] The abbreviations used are: AD, Alzheimer disease; SP, senile plaque; Aβ, amyloid β-peptide; APP, amyloid precursor protein; CTF, C-terminal fragment of APP; AICD, APP intracellular domain; ROS, reactive oxygen species; JNK, c-Jun N-terminal protein kinase; ERK, extracellular signal-regulated kinase; PKB, protein kinase B; siRNA, small interfering RNA; ELISA, enzyme-linked immunosorbent assay; DAPT, *N*-(*N*-(3,5-difluorophenacetyl)-L-alanyl)-*S*-phenylglycine *t*-butyl ester.

levels (18, 20), leading to an increase in amyloidogenic C-terminal fragment (C99) and Aβ levels *in vitro*. This suggests that H_2O_2 treatment leads to a shift in APP processing from the α-secretase to β-secretase pathway. In contrast, H_2O_2 also induces the production of intracellular Aβ by decreasing the protein levels of APP and C99, suggesting that excessive Aβ production may be caused by H_2O_2-facilitated APP processing (15). Whether the activity of γ-secretase is regulated by H_2O_2 is also poorly understood. Because the proteolysis of APP by γ-secretase is the last key step in Aβ generation, it is important to know whether and how endogenous γ-secretase activity is regulated during oxidative stress-inducing Aβ production.

Here, we show that H_2O_2 via c-Jun N-terminal kinase (JNK) enhances the activity of γ-secretase, leading to accelerated APP processing and Aβ accumulation. Our findings may provide a potential mechanism by which the stress-activated JNK contributes to senile plaque expansion and AD pathogenesis.

EXPERIMENTAL PROCEDURES

Plasmids—pcDNA3.1-APP695myc plasmid has been described previously (21). To generate pcDNA3.1-SP-C99myc expression vector, an 18-residue-long signal peptide was amplified by PCR from the human APP695 cDNA and introduced into HindIII and EcoRI sites, followed by ligation with C-terminal 99 amino acids (C99) of APP695 and Myc tag. AICDmyc-IRES2-EGFP construct was generated by PCR amplification from pcDNA3.1-APP695myc, introduced with an ATG start codon, and then cloned into the BglII and BamHI sites in the pIRES2-EGFP vector (Clontech). pcDNA3.0-C99-GVP, which encodes C99 fused with Gal4 DNA-binding/VP16 transactivation domains, was kindly provided by Dr. Helena Karlstrom (Medical Nobel Institute, Stockholm, Sweden) (22).

Site-directed Mutagenesis—Site-directed mutagenesis of APP695myc and SP-C99myc was conducted by PCR strategy (23). The paired mutagenic primers consist of primer forward (5′-TTGACGCCGCTGTCGCCCCAGAGGAGCGCCACCT-3′) and primer reverse (5′-GCTCCTC TGGGGCGACAGCG-GCGTCAACCTC-3′) with the underlined nucleotides indicating the changes introduced for the point mutations. The fidelity of entire coding sequences of above plasmids was confirmed by DNA sequencing.

Cell Culture and Treatments—Human embryonic kidney 293T cells (HEK293T) and human neuroblastoma cells (SH-SY5Y) were cultured in Dulbecco's modified Eagle's medium/Ham's F-12 (Sigma) with 10% fetal bovine serum (Hyclone). Transfection experiments were performed using FuGENE 6 (Roche Applied Science) in accordance with the manufacturer's instructions. To generate human neuroblastoma cell lines stably expressing APP695myc, SH-SY5Y cells were transfected with the construct and selected in the presence of G418 (500 μg/ml). SH-SY5Y/APP695myc cells were maintained in the medium containing 200 μg/ml of G418.

SH-SY5Y cells were routinely treated with 1.0 mM H_2O_2 for 1 h unless otherwise indicated in figure legends. Various pharmacological kinase inhibitors, *i.e.* SP600125 (20 μM; Calbiochem), U0126 (5 μM; Calbiochem), wortmannin (20 nM; Calbiochem), and γ-secretase inhibitor DAPT (1–10 μM; Sigma), were added into Dulbecco's modified Eagle's medium/Ham's F-12 medium for 3 h before H_2O_2 treatment.

RNA Interference—Silencing of JNK was achieved by transfection with Stealth siRNA duplexes targeting JNK1 or JNK2 (24). siJNK1 (5′-UCACAGUCCUGAAACGAUAtt-3′) targets *Jnk1* and siJNK1/2 (5′-AAAGAAUGUCCUACCUUCU tt-3′) targets a common sequence in both *Jnk1* and *Jnk2* mRNA. siCtrl (5′-CUUACGCUGAGUACU UCGAtt-3′) against luciferase was used as nonspecific siRNA control. All siRNAs were chemically synthesized by Shanghai GeneChem Co., Ltd. HEK293T cells in 12-well cell dish were co-transfected with 50 pmol of siRNA and 1.5 μg of pcDNA3.1-APP695myc with Lipofectamine2000 (Invitrogen). The cells were treated and harvested for immunoblot analysis 48 h later.

Aβ ELISA—To determine the production of intracellular Aβ, SH-SY5Y/APP695myc cells, or pcDNA3.1-SP-C99myc transiently expressed HEK293T cells were treated with 1.0 mM H_2O_2 for 1 h. The cells were lysed with cold radioimmune precipitation assay buffer containing 50 mM Tris-HCl (pH 8.0), 150 mM NaCl, 5 mM EDTA, 1% Nonidet P-40, 0.25 mM phenylmethanesulfonyl fluoride, and a mixture of protease inhibitors (Roche Applied Science). The cell extracts were centrifuged at 13,000 × *g* for 30 min to remove cell debris. The same amounts of protein extracts were subjected to sandwich Aβ ELISA kits according to the manufacturer's instruction (Biosource). To detect secreted $Aβ_{40}$ and $Aβ_{42}$, conditioned medium of H_2O_2-treated cells (300 μl/well) was collected to measure Aβ levels as above.

Immunoblot Analysis—The cells or tissues were lysed in cell lysis buffer containing 50 mM Tris-HCl (pH 8.0), 150 mM NaCl, 0.5% NaDOC, 0.1% SDS, 1% Nonidet P-40, 5 mM EDTA, 0.25 mM phenylmethanesulfonyl fluoride, and a mixture of protease inhibitors. Protein extracts (30 μg) were subjected to immunoblotting with the following primary antibodies: anti-Myc (1:3,000; Covance), anti-phospho-JNK (1:1,000; Cell Signaling), anti-pan JNK (1:2,000; PharMingen), anti-phospho-ERK (1:2,000; Cell Signaling), anti-ERK (1:1,000; Santa Cruz), anti-phospho-PKB (1:1,000; Santa Cruz), anti-PKB (1:1,000; Santa Cruz), and anti-β-actin (1:7,000; Sigma). To detect $sAPP_α$ and $sAPP_β$, conditioned medium of H_2O_2-treated cells was collected and analyzed by immunoblotting using the following primary antibodies: 22C11 recognizing APP N-terminal amino acid residues 66–81 (1:2,000; Chemicon), 6E10 reacting with the $Aβ_{4-9}$ region in the C terminus of $sAPP_α$ (1:1,000; Signet Laboratory), and anti-$sAPP_β$ antibody recognizing the potion of C terminus of human $sAPP_β$ (ISEVKM) (1:200; IBL). Antibody-reacted proteins were visualized using the ECL detection reagents. The autoradiography of x-ray film and the band intensity were processed using LabWorks software version 4.5 (UVP).

Fluorogenic Substrate Assay—Fluorogenic substrate assay was performed as described previously (25). In brief, H_2O_2-treated cells were homogenized in 50 mM HEPES (pH 7.4), 150 mM NaCl, 1 mM EDTA solution. The homogenate was centrifuged for 15 min at 1,000 × *g* at 4 °C to prepare a post-nuclear supernatant fraction. The cell membranes were pelleted from the post-nuclear supernatant by centrifugation for 30 min at 13,000 × *g*. The pellet was resuspended and incubated at 37 °C

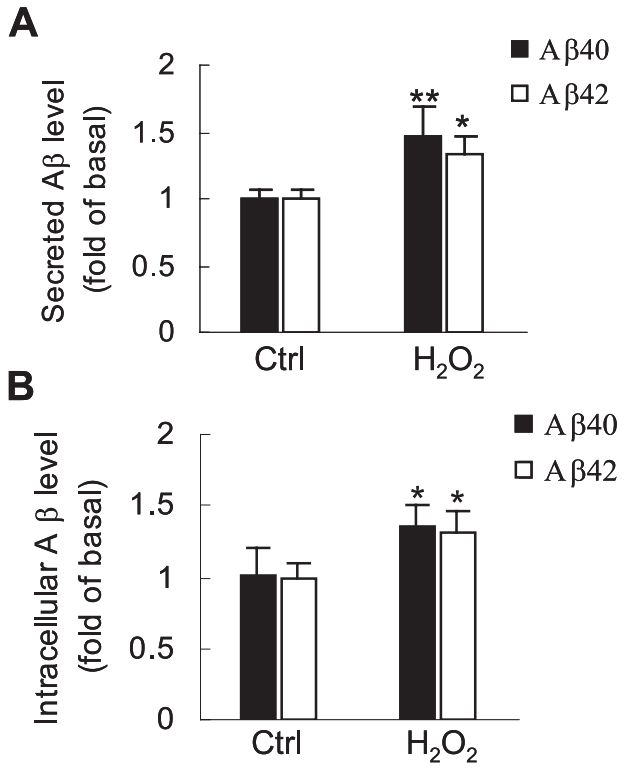

FIGURE 1. **H_2O_2 significantly induces intracellular and secreted Aβ.** *A*, SH-SY5Y/APP695myc cells were treated with 1.0 mM H_2O_2 in serum-free medium for 1 h or left untreated as indicated. Conditioned medium was collected and analyzed by sandwich Aβ ELISA to measure secreted $Aβ_{40}$ and $Aβ_{42}$ level. *B*, SH-SY5Y/APP695myc cells were lysed in ice-cold radioimmune precipitation assay buffer, and the same cell extracts were subjected to Aβ ELISA. *Ctrl*, control.

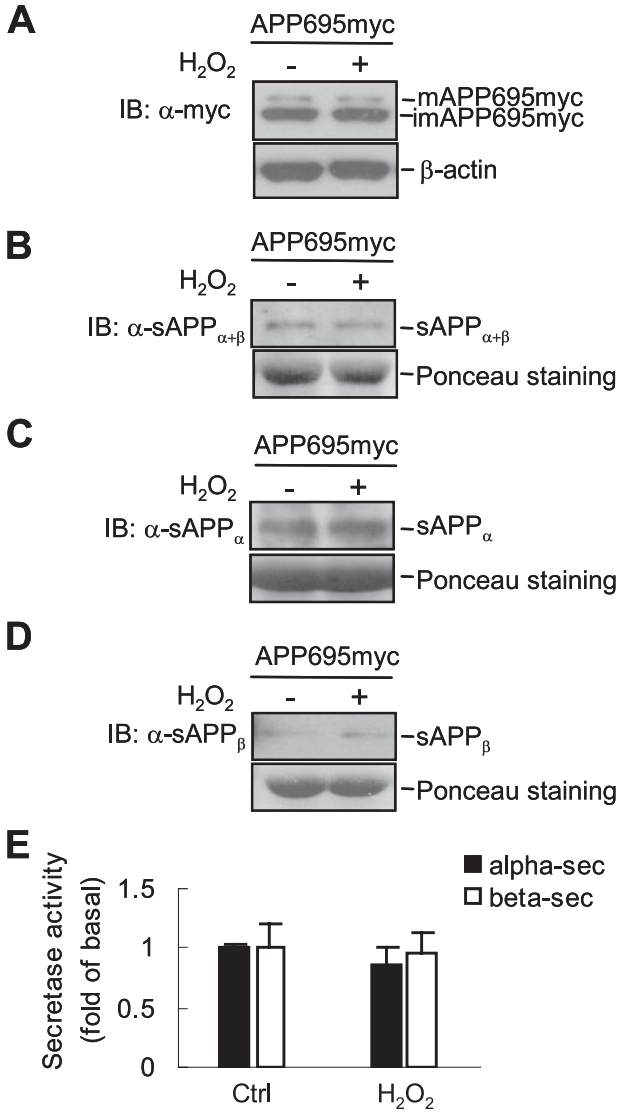

FIGURE 2. **H_2O_2 does not induce APP expression or stimulate the activity of α- and β-secretase.** *A*, after H_2O_2 treatment, SH-SY5Y/APP695myc cells were analyzed by immunoblotting (*IB*) using anti-Myc antibody. *B–D*, conditioned medium was collected and analyzed by immunoblotting, using 22C11 antibody to detect total sAPP (*B*), 6E10 antibody to detect $sAPP_α$ (*C*), and anti-$sAPP_β$ antibody to detect $sAPP_β$ (*D*). Loading controls (*Ctrl*) of conditioned medium were analyzed by Ponceau staining. *E*, determination of α- and β-secretase activity by fluorogenic substrate assays. Lysates of H_2O_2-treated cells were incubated with secretase substances at 37 °C for 2 h, and emission was measured.

for 2 h in 30 μl of reaction buffer (α-secretase reaction buffer: 100 mM sodium acetate, pH 7.0; β-secretase reaction buffer: 100 mM sodium acetate, pH 4.5) containing 2 μg of fluorogenic substrates (Calbiochem). The fluorescence values were measured by SpectraMax M5 spectrometer (Molecular Devices) with an excitation wavelength at 340 nm and an emission wavelength at 490 nm.

Cell-based γ-Secretase Assay—The activity of endogenous γ-secretase was measured by C99-Gal4/VP16 luciferase reporter assay as described previously (22). For each well of the 24-well cell culture plate, 100 ng of C99-GVP, 200 ng of pFR-Luc (Stratagene) and 50 ng of pRL-TK plasmids (Promega) were co-transfected into HEK293T cells. DAPT was added into cell medium at a final concentration of 10 μM for 12 h. The cells were stimulated with H_2O_2 for 1 h and analyzed for luciferase activity with the dual luciferase reporter system using a luminometer (Promega). The transfection efficiency was normalized by *Renilla* luciferase.

Human Brain Tissues Acquisition—Fresh frozen human cortex tissues from four individuals with AD and four age-matched nondemented control individuals were obtained via the rapid autopsy system of the Netherlands Brain Bank, Netherlands Institute for Neuroscience, Amsterdam, The Netherlands, which supplies post-mortem specimens from clinically well documented and neuropathologically confirmed cases. All of the material was collected from donors from whom a written informed consent for brain autopsy, and the use of the material and clinical information for research purposes had been obtained by the Netherlands Brain Bank. The research protocol with human tissues in this study was reviewed and approved by the Review Board of Shanghai Institutes for Biological Sciences, Chinese Academy of Sciences.

Immunofluorescence—Twelve-month old Tg2576 mice (26) and control nontransgenic littermates were perfused after deep anesthesia. The brains were fixed in phosphate-buffered saline containing 4% *para*-formaldehyde for 4 h, followed by the equilibration in 20% sucrose overnight at 4 °C. Embedded tissues were cryosectioned coronally into 10-μm sections and treated with 70% formic acid for 15 min, followed by immunostaining. The primary antibodies were anti-phospho-JNK (1:600) and 6E10 (1:300). Secondary antibodies were Cy3-con-

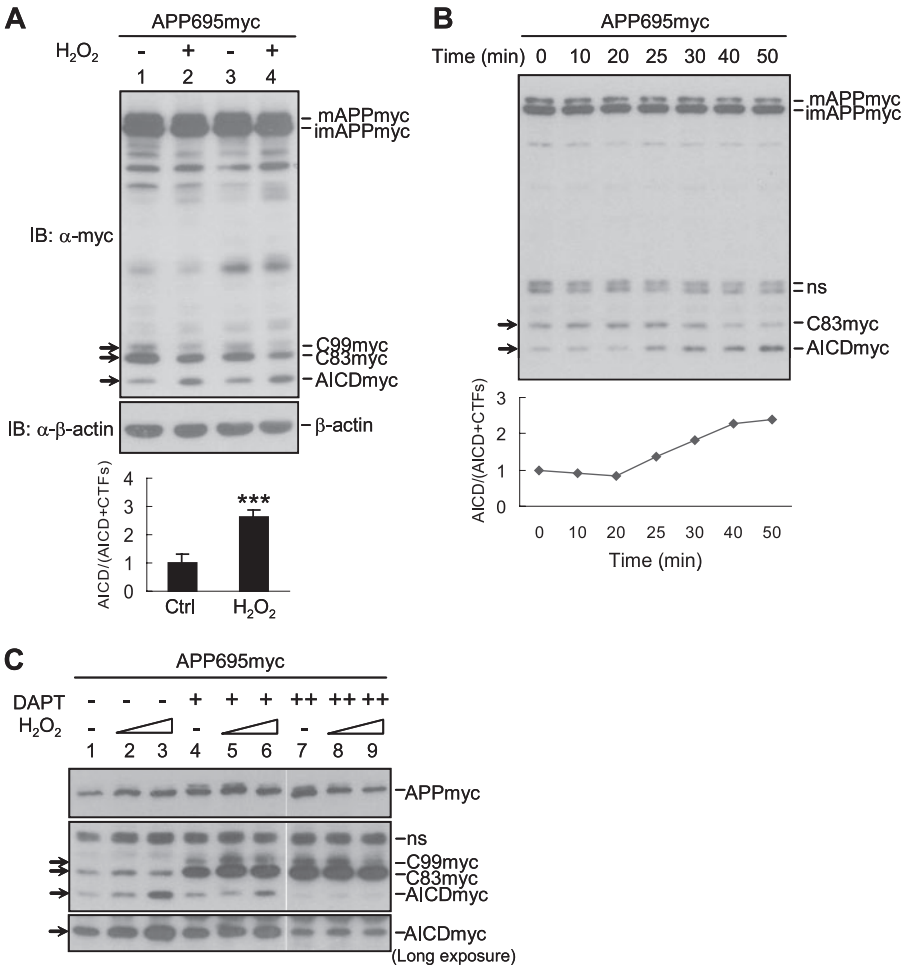

FIGURE 3. **H_2O_2 promotes γ-secretase-mediated processing of APP.** *A*, SH-SY5Y/APP695myc cells were treated with 1.0 mM H_2O_2, followed by immunoblotting (*IB*) using anti-Myc antibody. Quantification of AICD and CTFs was performed through normalization of APP level (*bottom panel*). *B*, a time course of H_2O_2-induced γ-secretase-mediated APP processing. The cells were treated with H_2O_2 up to 50 min and harvested at indicated time points. APP processing was analyzed as described in *A*. *C*, cells were pretreated with the γ-secretase inhibitor DAPT (1 and 10 μM) or the control Me_2SO for 3 h, followed by H_2O_2 treatment. APP processing was monitored by immunoblotting as described in *A*. *ns*, nonspecific.

jugated goat anti-rabbit IgG (1:500; Jackson ImmunoResearch Laboratories) and fluorescein isothiocyanate-conjugated goat anti-mouse IgG (1:500; Jackson ImmunoResearch Laboratories). Normal rabbit IgG (1:500; Zymed Laboratories Inc.) was used as the negative control. 4′,6′-Diamino-2-phenylindole (1:2,000; Sigma) was applied for detecting cell nucleus. The images were taken with Olympus BX50 fluorescence microscopy and Leica DM RE confocal microscopy.

Statistics—Each experiment was repeated at least three times. The data were expressed as the means ± S.D. Student's *t* tests were used to compare the effects of all treatments. The differences were considered statistically significant as: *, $p < 0.05$; **, $p < 0.01$; and ***, $p < 0.001$.

RESULTS

H_2O_2 Enhances Intracellular and Secreted Aβ—Previous studies have shown that the level of ROS was abnormally high in brain areas that surround senile plaques, because of microglia activation or Aβ accumulation (12, 13). H_2O_2 is an important endogenous product of ROS and is often used as a pro-oxidant *in vitro* studies (27). To determine whether a high level of ROS affects Aβ generation, SH-SY5Y/APP695myc cells were treated with 1 mM H_2O_2. Aβ ELISA showed that H_2O_2 significantly increased the level of $Aβ_{40}$ and $Aβ_{42}$ in cell culture medium when compared with the control (Fig. 1*A*). To determine that Aβ accumulation in cell medium was a result of enhanced Aβ generation but not facilitated Aβ secretion, intracellular $Aβ_{40}$ and $Aβ_{42}$ in H_2O_2-treated cells were also measured. We found that H_2O_2 also significantly increased the level of intracellular $Aβ_{40}$ and $Aβ_{42}$ (Fig. 1*B*). Taken together, these data indicate that pro-oxidant H_2O_2 elevates intracellular Aβ generation and increases its accumulation in cell culture medium.

H_2O_2 Has No Effect on APP Expression or α/β-Secretase Activity—Aβ derives from its precursor APP through two proteolytic events that are mediated by β- and γ-secretase. Deregulation of APP processing can cause Aβ dysmetabolism, leading to pathological deposition (4). To study the underlying mechanism of H_2O_2-induced Aβ production, we first determined whether H_2O_2 induces APP expression, thereby promoting Aβ production. Immunoblot analysis showed that there were no detectable changes in the level of mature or immature APP695 proteins in SH-SY5Y/APP695myc cells upon H_2O_2 treatment (Fig. 2*A*), suggesting that enhanced Aβ was not caused by alteration of APP synthesis or maturation.

Next we examined the activity of α- and β-secretase in response to H_2O_2 treatment by measuring the products of α- and β-secretase-mediated APP cleavage ($sAPP_α$ and $sAPP_β$) (28). We used anti-APP antibody (22C11) and found that there were no detectable changes in total soluble APP ($sAPP_{α+β}$) (Fig. 2*B*). Neither the level of $sAPP_α$ nor $sAPP_β$ was affected by H_2O_2, as analyzed by immunoblotting using 6E10 and anti-$sAPP_β$ antibodies, which recognize $sAPP_α$ and $sAPP_β$ in the cell medium, respectively (Fig. 2, *C* and *D*). Similar results were obtained when the activity of α- or β-secretase was measured by fluorogenic substrate assay (Fig. 2*E*). Thus, H_2O_2 does not significantly affect APP expression or the activity of α- and β-secretase.

H_2O_2 Promotes γ-Secretase-mediated APP695 Cleavage—In addition to α- and β-secretase, γ-secretase is another key secretase that directly determines Aβ production (5). To determine whether γ-secretase-mediated APP cleavage is stimulated by

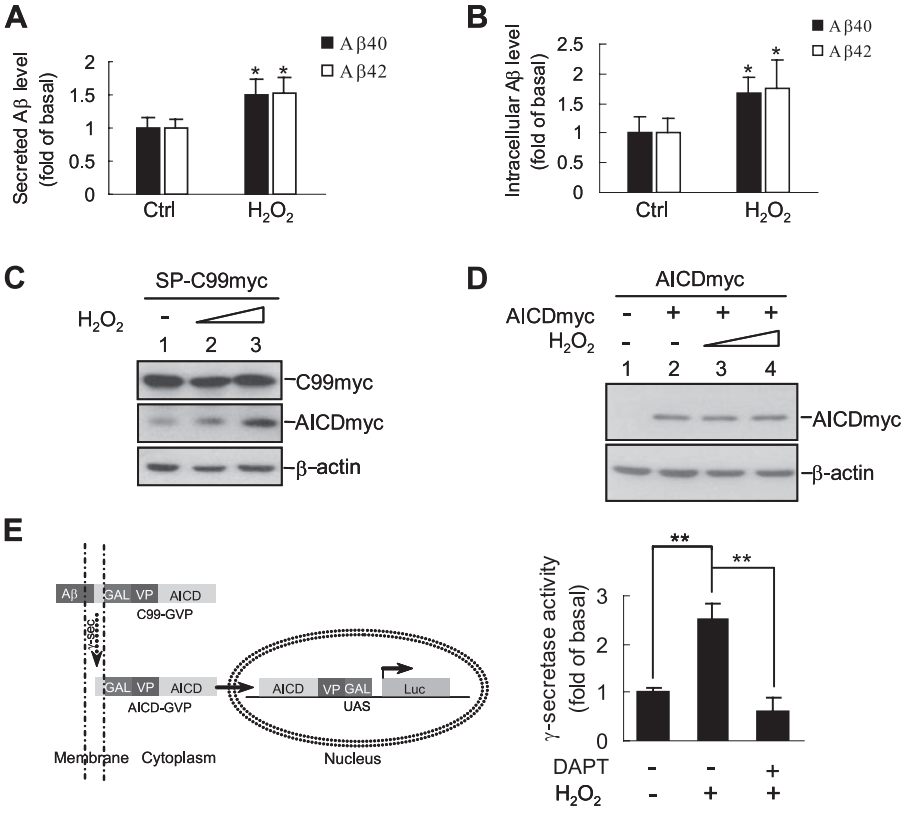

FIGURE 4. **H_2O_2 promotes γ-secretase-mediated SP-C99myc processing.** *A*, determination of H_2O_2-induced secreted $A\beta_{40}$ and $A\beta_{42}$ production. HEK293T cells were transiently transfected with pcDNA3.1-SP-C99myc for 24 h. Conditioned medium of H_2O_2-treated cells was collected and analyzed by ELISA to measure secreted $A\beta_{40}$ and $A\beta_{42}$ levels. *B*, determination of intracellular $A\beta_{40}$ and $A\beta_{42}$ levels in above cells. *C*, immunoblotting analysis of H_2O_2-induced AICD production in a dose-dependent manner in above cells (0.2 and 1.0 mM H_2O_2). *D*, HEK293T cells were transfected with pcDNA3.1-AICDmyc or empty vector and treated with various doses of H_2O_2 (0.2 and 1.0 mM H_2O_2). AICD accumulation was analyzed by immunoblotting using anti-Myc antibody. *E*, schematic representation of γ-secretase-dependent luciferase reporter assay (*left panel*). HEK293T cells were co-transfected with expression plasmids encoding C99-GVP, pFR-luc, and pRL-TK. The cells were pretreated with DAPT (10 μM) for 12 h, followed by H_2O_2 for another hour. Relative luciferase activity was analyzed as described under "Experimental Procedures" (*right panel*). *Ctrl*, control.

H_2O_2, thereby promoting Aβ production, we examined APP processing by immunoblotting. As previously reported (29), the expression level of APP695 in SH-SY5Y cells was quite abundant, and it was cleaved by α- or β-secretase into a small quantity of CTFs (including C83 and C99) spanning in the membrane. CTFs were further hydrolyzed by γ-secretase, releasing APP intracellular domain (AICD) into cytoplasm (supplemental Fig. S1*A*). With exposure to H_2O_2, we found that both C99 and C83 were decreased, whereas AICD was evidently elevated (Fig. 3*A*, compare *lanes 1* and *3* with *lanes 2* and *4*). A time course study revealed that CTFs in SH-SY5Y/APP695myc cells were reduced gradually, accompanied with the increase in AICD. H_2O_2 induced the conversion of C83 to AICD as early as 25 min after H_2O_2 treatment (Fig. 3*B*).

Because AICD is derived from γ-secretase-dependent cleavage of CTFs, the ratio of AICD/(AICD+CTFs) might represent the efficiency of γ-secretase-mediated hydrolysis reaction. Quantification of CTFs and AICD bands intensity showed that there was a significant increase in AICD/(AICD+CTFs) between control and H_2O_2-treated cells (Fig. 3*A*, *bottom panel*). To determine whether γ-secretase is involved in H_2O_2-induced conversion of CTFs to AICD, SH-SY5Y/APP695myc cells were pretreated with a specific γ-secretase inhibitor, DAPT, before H_2O_2 treatment. Indeed, the H_2O_2-enhanced AICD level was decreased after 1 μM DAPT pretreatment (Fig. 3*C*, compare *lanes 4–6* with *lanes 1–3*), and AICD was effectively reduced to the basal level with a higher concentration (10 μM) of DAPT pretreatment (Fig. 3*C*, compare *lanes 7–9* with *lanes 1–3*). The identity of the bands recognized by the anti-Myc antibody was further validated by immunoblotting analysis with anti-APP C-terminal antibody (anti-APP676–695) (supplemental Fig. S1*B*). In addition, H_2O_2 could promote γ-secretase-mediated normal untagged APP695 processing by reducing C83 levels also (supplemental Fig. S1*C*), although we were unable to detect AICD band because it was degraded very quickly without Fe65 stabilization (30). Thus, H_2O_2 appears to promote γ-secretase-mediated APP processing.

H_2O_2 Enhances γ-Secretase-mediated C99 Processing—C99, which is generated from β-secretase-mediated cleavage of APP695, is a direct substrate of γ-secretase and an immediate precursor of Aβ (31). To further determine whether H_2O_2 induces Aβ elevation through activation of γ-secretase, but not α- or β-secretase, HEK293T cells were transfected with pcDNA3.1-SP-C99myc to replace full-length APP695. Consistent with the results obtained from APP695, ELISA showed that H_2O_2 induced a significant increase in secreted $A\beta_{40}$ and $A\beta_{42}$ in cell culture medium (Fig. 4*A*). Similar results were obtained with intracellular $A\beta_{40}$ and $A\beta_{42}$ (Fig. 4*B*).

In addition, Western blot showed that the other product of γ-secretase-mediated cleavage of C99, AICD, was also correspondingly increased in a dose-dependent manner upon H_2O_2 treatment (Fig. 4*C*). To exclude the possibility that the H_2O_2-elevated AICD level is caused by the impairment of AICD degradation, HEK293T cells were transiently transfected with expression plasmids encoding AICDmyc, and its yield was analyzed after H_2O_2 treatment. Immunoblotting analysis showed that there was no significant difference in AICD level between control and H_2O_2-treated cells (Fig. 4*D*). When new AICD generation was blocked by 10 μM DAPT, H_2O_2 did not induce accumulation of remaining AICD (Fig. 3*C*, *lanes 7–9*, long exposure, *bottom panel*). These data suggest that H_2O_2 did not prevent AICD from degradation.

We next used a cell-based reporter gene assay to measure the endogenous γ-secretase activity (22). Transfection of either C99-GVP or pFR-luc plasmids into HEK293T cells could not activate the reporter gene, but co-transfection of these two constructs

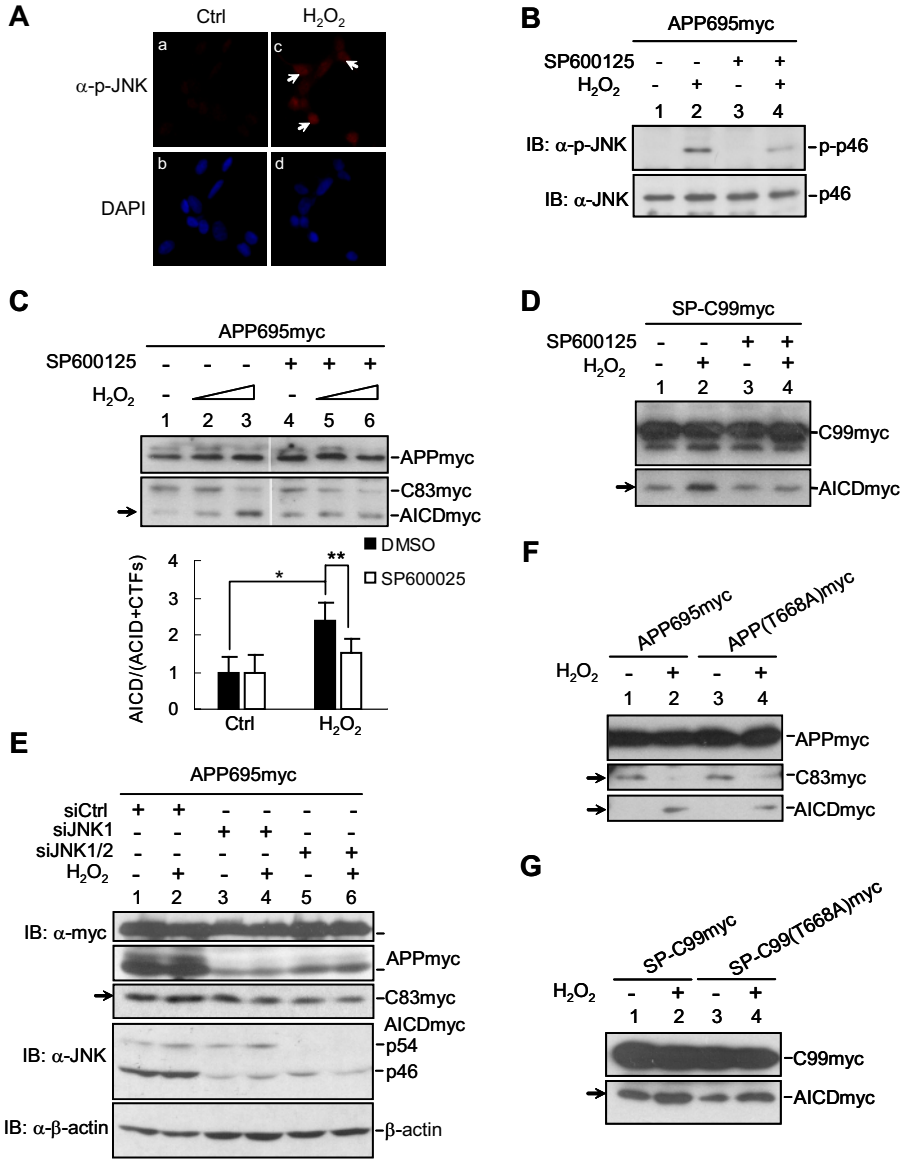

FIGURE 5. **H_2O_2 promotes γ-secretase-mediated APP cleavage through JNK activation.** *A*, immunofluorescent staining of JNK activation in H_2O_2-treated SH-SY5Y cells. *B*, immunoblot (*IB*) analysis of H_2O_2-induced JNK activation in SH-SY5Y cells. The cells were serum-starved for 12 h and pretreated with JNK inhibitor SP600125 (20 μM) or Me_2SO control (*Ctrl*) for 3 h. After incubation with H_2O_2 for 15 min, the cells were harvested, and JNK activation was analyzed by immunoblotting with anti-phospho-JNK antibody. *C*, determination of the inhibitory effect of SP600125 on γ-secretase-mediated cleavage of APP695myc in H_2O_2-treated SH-SY5Y/APP695myc cells. *D*, determination of the inhibitory effect of SP600125 on γ-secretase-mediated cleavage in H_2O_2-treated HEK293T/SP-C99myc cells. *E*, the effect of siJNK on H_2O_2-induced γ-secretase-mediated APP cleavage. HEK293T cells were co-transfected with APP695myc and siRNA against *Jnk1* or *Jnk1/2*. After H_2O_2 stimulation, the cells were analyzed by immunoblotting. *F* and *G*, immunoblot analysis of H_2O_2 effect on the processing of APP695myc(T668A) mutant (*F*) or SP-C99myc(T668A) mutant (*G*).

could activate the luciferase gene expression, indicating that luciferase activity was controlled by endogenous γ-secretase-mediated C99 cleavage (Fig. 4*E*, *left panel*). When C99-GVP and pFR-luc co-transfected cells were treated with H_2O_2, the luciferase activity was significantly increased compared with controls. This increase, however, was abolished by pretreatment of γ-secretase inhibitor DAPT (Fig. 4*E*, *right panel*). Thus, H_2O_2 promotes C99 cleavage by activating endogenous γ-secretase.

H_2O_2 Promotes γ-Secretase-mediated APP Cleavage through JNK Activation—It has been shown that H_2O_2 activates JNK, one of the mitogen-activated protein kinases that is readily activated in response to various environmental stresses, to decide the fate of cells (32). To test whether JNK is involved in activation of γ-secretase by H_2O_2, we first determined the stimulatory effect of H_2O_2 on JNK in SH-SY5Y cells. Immunofluorescence staining and Western blot using anti-phospho-JNK antibody showed that JNK was phosphorylated at Thr^{183} and Tyr^{185} in the activation T-loop in cells treated with H_2O_2 when compared with that in control cells (Fig. 5, *A* and *B*, *lane 2*), as well as in HEK293T cells (data not shown). Consistently, pretreatment with JNK inhibitor SP600125 also decreased JNK activation (Fig. 5*B*, *lane 4*).

Next, we wondered whether JNK activation is required for H_2O_2 to promote γ-secretase-mediated APP cleavage. SH-SY5Y/APP695myc cells were pretreated with or without SP600125 for 3 h, followed by H_2O_2 treatment. H_2O_2 induced γ-secretase-dependent AICD production in control cells (Fig. 5*C*, compare *lane 3* with *lane 1*) but was unable to do so in cells pretreated with SP600125 (Fig. 5*C*, compare *lane 6* with *lane 4*). The pretreatment with SP600125 significantly reduced the ratio of H_2O_2-induced AICD/(AICD+CTFs), as measured by the intensity of signals (Fig. 5*C*, *bottom panel*). Similarly, the pretreatment with SP600125 also reduced H_2O_2-indcued AICD to basal level in HEK293T cells transiently transfected with SP-C99myc (Fig. 5*D*, compare *lane 4* with *lane 2*). Furthermore, silencing of JNK expression by siJNKs (24), which efficiently reduced the endogenous JNK protein level (Fig. 5*E*) but not the control siRNA, decreased H_2O_2-induced AICD level (Fig. 5*E*, compare *lanes 4* and *6* to *lane 2*). Taken together, these data show that activation of JNK is required for H_2O_2 to promote γ-secretase-mediated APP cleavage.

It has been reported that JNK can phosphorylate the γ-secretase substrate APP at Thr^{668}, thereby facilitating APP processing and Aβ production (33, 34). To determine whether Thr^{668} phosphorylation of APP accounts for H_2O_2-induced JNK-dependent promotion of γ-secretase-mediated APP cleavage, HEK293T cells were transiently transfected with mammalian expression plasmids encoding wild type APP695myc or

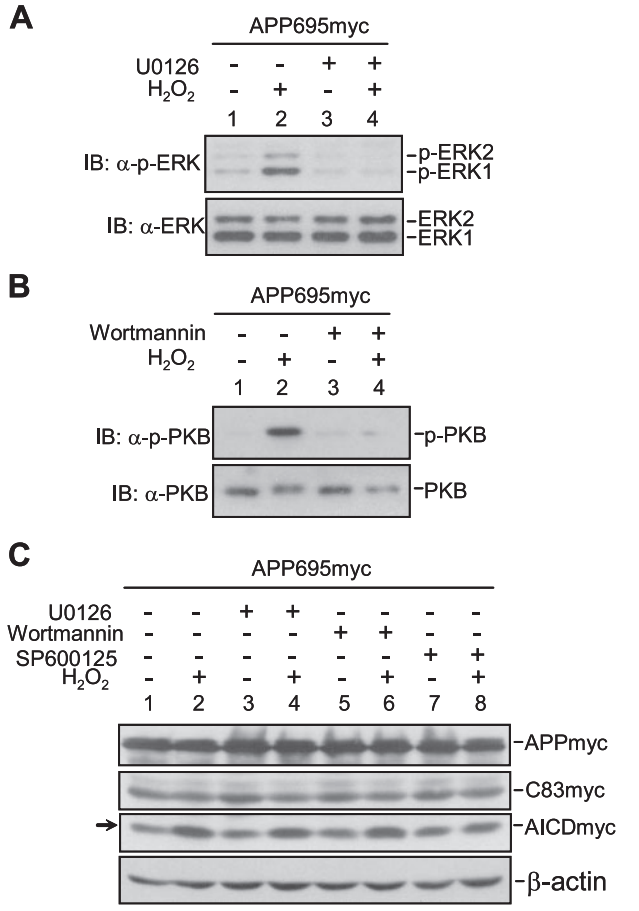

FIGURE 6. **JNK, but not ERK or PKB, is required for H_2O_2 to promote γ-secretase-mediated APP cleavage.** The cells were serum-starved for 12 h and pretreated with U0126 (5 μM) (*A*), wortmannin (20 nM) (*B*), SP600125 (20 μM) (*C*) or the control Me_2SO for 3 h. After H_2O_2 treatment, the cells were analyzed by immunoblotting (*IB*) to determine the effect of the above inhibitors on activation of ERK (*A*), PKB (*B*), and APP processing (*C*).

APP(T668A)myc, in which Thr^{668} has been replaced by Ala^{668}. Immunoblot analysis showed that in both wild type and T668A mutant transfected cells, AICD products were elevated, whereas CTFs products decreased after H_2O_2 stimulation (Fig. 5*F*, *lanes 3* and *4*). Consistently, H_2O_2 also increased AICD level in HEK293T cells expressing SP-C99myc mutant (Fig. 5*G*, *lanes 3* and *4*). The similarity of proteolytic process between wild type APP and APP(T668A) mutant suggests that H_2O_2-induced, JNK-dependent augmentation of γ-secretase-mediated APP cleavage is likely due to activation of the γ-secretase rather than Thr^{668} phosphorylation of APP.

JNK, but Not ERK or PKB, Is Required for H_2O_2 to Promote γ-Secretase-mediated APP Cleavage—H_2O_2 activates multiple downstream signal pathways (35). We found that in addition to JNK, ERK and PKB were activated by H_2O_2 (Fig. 6, *A* and *B*). To determine whether JNK is mainly responsible for H_2O_2-induced augmentation of γ-secretase activity, we used specific pharmacological inhibitors to inhibit individual kinases. Immunoblot analysis showed that ERK and PKB were significantly inhibited by U0126 or wortmannin, respectively (Fig. 6, *A* and *B*). However, only SP600125, but not U0126 or wortmannin, was able to inhibit H_2O_2-induced augmentation of AICD production (Fig. 6*C*). Thus, these data suggest that H_2O_2 enhances endogenous γ-secretase activity through activation of JNK.

TABLE 1
Case details of AD patients and control subjects from the Netherlands Brain Bank

Group	Gender	Age	Pmd[a]	pH	Brain weight	Region
			h		*g*	
Alzheimer disease						
A1	M	92	3:30	7.2	1175	Medial frontal gyrus
A2	F	94	2:55	6.53	955	Superior temporalis gyrus
A3	F	80	2:20	6.41	1030	Superior temporalis gyrus
A4	F	78	6:35	7	1084	Angular gyrus
Nondemented control						
N1	M	88	7:00	6.84	1398	Medial frontal gyrus
N2	F	78	6:25	6.5	1135	Inferior temporalis gyrus
N3	F	73	5:30	6.38	1304	Superior temporalis gyrus
N4	F	74	5:35	7.04	982	Angular gyrus

[a] Pmd, postmortem delay.

JNK Is Activated in Brain Areas Surrounding Senile Plaques of AD Animal Model—To investigate the relation between JNK and Aβ production *in vivo*, we examined JNK activation in brain tissues of AD patients. Hippocampus and cortices of human brain tissues from AD patients ($n = 4$) and nondementional controls ($n = 4$) were examined for JNK activation (Table 1). The level of phosphorylated JNK was evidently increased in the brains of AD patients when compared with control brains, whereas there was no significant difference in JNK expression level (Fig. 7*A*), consistent with previous reports (36, 37).

To determine the link between amyloid deposits and JNK activation, we performed an immunostaining in brains of the AD animal model (Tg2576 mice) and found that phospho-JNK immunoreactivity was localized in the surrounding region of senile plaques, which was positive with Aβ antibody 6E10 (Fig. 7*B*, *panels a*, *b*, and *d*). In contrast, both senile plaques and phospho-JNK were negative in the brains of control nontransgenic littermates (data not shown). The immunostaining of JNK by the anti-phospho-JNK antibody was highly specific, because normal rabbit IgG was unable to detect any phospho-JNK immunoreactivity (Fig. 7*B*, *panel f*). The core of amyloid deposits was 4′,6′-diamino-2-phenylindole-negative (Fig. 7*B*, *panels c* and *g*), suggesting that cells were dead and lost in the area of amyloid deposited. Taken together, these results show that activation of JNK is related to amyloid deposits *in vivo*.

DISCUSSION

Oxidative stress has been implicated in the pathogenesis of AD, because it induces Aβ production and contributes to Aβ neurotoxicity (12–15, 19). Yet the underlying mechanism is not completely understood. In this study, we report that the prooxidant H_2O_2 promotes Aβ production through JNK-dependent activation of γ-secretase.

The APP processing is a sequential proteolysis that is carried out by β- and γ-secretase, which leads to the generation of Aβ and ultimately neurotoxicity (4). Not surprisingly, the processing of APP is tightly regulated. Although it has been reported that oxidative stress can induce Aβ production, it is not clear whether γ-secretase activity is regulated by oxidative stress and, if so, what the underlying mechanism is (15–18, 20). We found

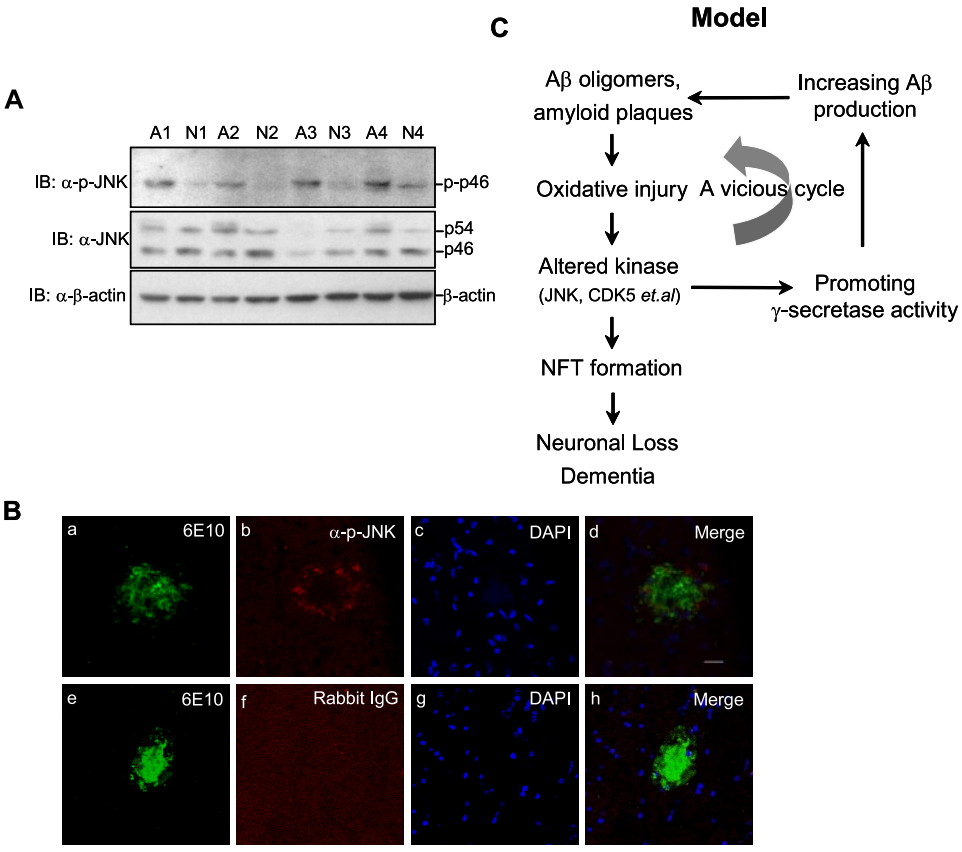

FIGURE 7. **JNK is activated in the brain areas that surround senile plaques *in vivo*.** *A*, human brain samples (30 μg of total protein extracts) from AD ($n = 4$) and age-matched control samples ($n = 4$) were analyzed for JNK activation using anti-phospho-JNK and anti-pan JNK antibodies. *B*, immunostaining of active JNK and senile plaques in Tg2576 mouse brain. Sections were stained with 6E10 (*green*, *panels a* and *e*) and anti-phospho-JNK antibody (*red*, *panel b*). Normal rabbit IgG was used as a negative control of anti-phospho-JNK (*panel f*). The nucleus was indicated with 4′,6′-diamino-2-phenylindole (*DAPI*, *blue*, *panels c* and *g*). The *scale bar* represents 20 μm. *C*, the model of H_2O_2 via JNK promotes γ-secretase-mediated APP processing. See "Discussion " for the details. *IB*, immunoblotting.

that H_2O_2 induced Aβ production through enhancement of γ-secretase activation, resulting in promotion of APP cleavage. First, H_2O_2 induced a significant increase in AICD without the inhibition on AICD degradation (Figs. 3 and 4). This notion is also supported by the observation that the substrates of γ-secretase, CTFs, were decreased accordingly (Fig. 3). Second, H_2O_2-induced increase in AICD was blocked by DAPT, the inhibitor of γ-secretase (Fig. 3). Third, H_2O_2 accelerated SP-C99 processing, which was only determined by γ-secretase without β-secretase interference (Fig. 4). This excludes the possibility that the increase of Aβ is due to the enhanced β-secretase activity to elevate C99 level. In contrast to previous reports (16–18, 20), immunoblot analysis and fluorogenic substrate assay showed that APP expression or β-secretase activity was not affected by H_2O_2 treatment (Fig. 2). The apparent discrepancy may be caused by the dose and duration of H_2O_2 treatment. In the previous reports, changes in APP expression or β-secretase activity occurred several hours after the cells were treated with a low concentration of H_2O_2 (16, 17). However, we found that γ-secretase-mediated APP cleavage was not affected by a low concentration of H_2O_2 (from 1 to 100 μM; data not shown). Although the exact concentration of H_2O_2 *in vivo* is unknown, it has been reported that 100 μM is the possible concentration under physiological conditions (38). Under pathological conditions, however, the concentration of ROS may be much higher (39). To defend a host against microbial organism infections, immune cells may need to generate millimolar quantities of H_2O_2 (27, 40, 41). Patients with vitiligo accumulate millimolar concentration of H_2O_2 in their epidermis (42, 43). In the brains of AD patients, microglia is activated, and inflammation occurs around the senile plaques (44), which might produce large amounts of H_2O_2. Another source of H_2O_2 might be from the progression of Aβ aggregation (14). It is consistent with the observation that ROS is abnormally higher in the AD patients, especially in the senile plaque-surrounding areas, than that in normal elder people, (12, 13). Thus, the high concentration of H_2O_2 (mM) used in this study might mimic the pathological conditions of the limited areas that surround the senile plaques. Taken together, our results show that H_2O_2 promotes γ-secretase-mediated APP cleavage, thereby contributing to Aβ production. Whether H_2O_2 also inhibits Aβ degradation needs to be determined in future studies.

H_2O_2 activates multiple signaling pathways, including ERK, PKB, and JNK (35). Our data show that only JNK is required for H_2O_2-induced activation of γ-secretase. First, immunofluorescent staining and immunoblotting showed that JNK was activated in the H_2O_2-treated SH-SY5Y cells (Fig. 5). Second, the JNK inhibitor SP600125, but not the inhibitors of ERK and PKB, specifically blocked H_2O_2-promoted γ-secretase-mediated cleavage of APP or C99 (Figs. 5 and 6). Third, JNK siRNA efficiently reduced H_2O_2-induced AICD levels (Fig. 5). These observations are consistent with a previous finding that proinflammatory cytokine-activated JNK also contributes to γ-secretase activity and Aβ production in HEK293 cells (45). Thus, JNK may play a central role in mediating the stimulatory effect of different stress signals on γ-secretase activity under pathological conditions.

The molecular mechanism by which JNK regulates γ-secretase activity and APP processing remains to be determined. It is possible that JNK phosphorylates APP and thereby makes it a better substrate for γ-secretase (33, 34). However, this seems less likely because proteolysis of APP(T668A) mutant and SP-C99(T668A) mutants was still promoted by H_2O_2 in our study (Fig. 5). This suggests that H_2O_2-induced γ-secretase activation is likely independent of APP Thr^{668} phosphorylation. Whether other phosphorylation sites of APP are involved has yet to be determined. Another possibility is that JNK may

enhance the enzyme activity of γ-secretase through protein phosphorylation, either directly or indirectly. *In vitro* kinase assay showed that activated JNK directly phosphorylated presenilin 1, which is the core component of γ-secretase enzyme (supplemental Fig. S2). Future studies will reveal the relationship between γ-secretase phosphorylation and its enzyme activity.

It has been reported that a high concentration of H_2O_2 induces cell death via JNK activation (46). We found that H_2O_2-treated cells had typical characteristics of cell death, as analyzed by 3-(4,5-dimethylthiazol-2-yl)-2,5-diphenyltetrazolium bromide assay and trypan blue exclusion (data not shown). Furthermore, only SP600125, but not U0126 or wortmannin, protected cells from H_2O_2-induced morphological changes (supplemental Fig. S3). Thus, it is possible that H_2O_2-stimulated JNK contributes to cell death, which provides a subtle acid environment that is needed for γ-secretase aspartyl protease activity, resulting in enhanced Aβ production (47). This hypothesis is consistent with the report that Aβ products increase during cell death (48, 49). During the preparation of the current manuscript, it was reported that oxidative stress induces expression of β-secretase through JNK-dependent regulation of γ-secretase, thereby providing a forward feedback between γ- and β-secretase for the cleavage of APP (50). However, the underlying mechanism remains to be elucidated. Future studies are needed to test all of these possibilities.

The classical Aβ hypothesis states that excessive accumulation of Aβ in the brains of AD patients increases oxidative stress and activates protein kinases, resulting in neurofibrillary tangle formation and neuronal loss (1). We found that active JNK located around amyloid deposits in brains of AD mouse model (Fig. 7*C*), consistent with the previous report that JNK is strongly activated in mutant APP transgenic mice upon extensive oxidative damage but not in mutant APP transgenic mice with little oxidative damage (51). Thus, we hypothesize that at the modest and late stage of AD brains, escalated Aβ accumulation and microglia activation induce high level of ROS including endogenous H_2O_2. Excessive ROS stimulate JNK activity in susceptible neurons that surround the amyloid plaques. These cells in turn produce more Aβ peptide through JNK-dependent, γ-secretase-mediated APP cleavage. The resultant Aβ is secreted and deposited around the core of original plaque, leading to plaque expansion in the brains of AD patients. Such exacerbation of a vicious cycle may explain how the process of AD pathology becomes accelerated and irreversible at the modest and late AD stage (Fig. 7*C*). New therapeutic targets for the intervention of AD pathogenesis might be identified along this signaling cascade.

Acknowledgments—We are grateful to Drs. Helena Karlstrom, Christian Haass, Dai Zhang, and Inge Huitinga for providing constructs, cell lines, and human brain tissues.

REFERENCES

1. Selkoe, D. J. (2002) *Science* **298,** 789–791
2. Saido, T. C., and Iwata, N. (2006) *Neurosci. Res.* **54,** 235–253
3. Funato, H., Yoshimura, M., Kusui, K., Tamaoka, A., Ishikawa, K., Ohkoshi, N., Namekata, K., Okeda, R., and Ihara, Y. (1998) *Am. J. Pathol.* **152,** 1633–1640
4. Mattson, M. P. (2004) *Nature* **430,** 631–639
5. Selkoe, D. J., and Wolfe, M. S. (2007) *Cell* **131,** 215–221
6. Marjaux, E., Hartmann, D., and De Strooper, B. (2004) *Neuron* **42,** 189–192
7. Shah, S., Lee, S. F., Tabuchi, K., Hao, Y. H., Yu, C., LaPlant, Q., Ball, H., Dann, C. E., 3rd, Sudhof, T., and Yu, G. (2005) *Cell* **122,** 435–447
8. Wolfe, M. S., Xia, W., Ostaszewski, B. L., Diehl, T. S., Kimberly, W. T., and Selkoe, D. J. (1999) *Nature* **398,** 513–517
9. Edbauer, D., Winkler, E., Regula, J. T., Pesold, B., Steiner, H., and Haass, C. (2003) *Nat. Cell Biol.* **5,** 486–488
10. Koo, E. H., and Kopan, R. (2004) *Nat. Med.* **10,** (suppl.) S26–S33
11. Finkel, T., and Holbrook, N. J. (2000) *Nature* **408,** 239–247
12. Smith, M. A., Rottkamp, C. A., Nunomura, A., Raina, A. K., and Perry, G. (2000) *Biochim. Biophys. Acta* **1502,** 139–144
13. Ono, K., Hamaguchi, T., Naiki, H., and Yamada, M. (2006) *Biochim. Biophys. Acta* **1762,** 575–586
14. Tabner, B. J., El-Agnaf, O. M., Turnbull, S., German, M. J., Paleologou, K. E., Hayashi, Y., Cooper, L. J., Fullwood, N. J., and Allsop, D. (2005) *J. Biol. Chem.* **280,** 35789–35792
15. Misonou, H., Morishima-Kawashima, M., and Ihara, Y. (2000) *Biochemistry* **39,** 6951–6959
16. Frederikse, P. H., Garland, D., Zigler, J. S., Jr., and Piatigorsky, J. (1996) *J. Biol. Chem.* **271,** 10169–10174
17. Tong, Y., Zhou, W., Fung, V., Christensen, M. A., Qing, H., Sun, X., and Song, W. (2005) *J. Neural. Transm.* **112,** 455–469
18. Tamagno, E., Parola, M., Bardini, P., Piccini, A., Borghi, R., Guglielmotto, M., Santoro, G., Davit, A., Danni, O., Smith, M. A., Perry, G., and Tabaton, M. (2005) *J. Neurochem.* **92,** 628–636
19. Sung, S., Yao, Y., Uryu, K., Yang, H., Lee, V. M., Trojanowski, J. Q., and Pratico, D. (2004) *FASEB J.* **18,** 323–325
20. Tamagno, E., Bardini, P., Obbili, A., Vitali, A., Borghi, R., Zaccheo, D., Pronzato, M. A., Danni, O., Smith, M. A., Perry, G., and Tabaton, M. (2002) *Neurobiol. Dis.* **10,** 279–288
21. Tang, K., Wang, C., Shen, C., Sheng, S., Ravid, R., and Jing, N. (2003) *Eur. J. Neurosci.* **18,** 102–108
22. Karlstrom, H., Bergman, A., Lendahl, U., Naslund, J., and Lundkvist, J. (2002) *J. Biol. Chem.* **277,** 6763–6766
23. Cheng, L., Jin, Z., Liu, L., Yan, Y., Li, T., Zhu, X., and Jing, N. (2004) *FEBS Lett.* **565,** 195–202
24. Oleinik, N. V., Krupenko, N. I., and Krupenko, S. A. (2007) *Oncogene* **26,** 7222–7230
25. Ermolieff, J., Loy, J. A., Koelsch, G., and Tang, J. (2000) *Biochemistry* **39,** 12450–12456
26. Hsiao, K., Chapman, P., Nilsen, S., Eckman, C., Harigaya, Y., Younkin, S., Yang, F., and Cole, G. (1996) *Science* **274,** 99–102
27. Rhee, S. G. (2006) *Science* **312,** 1882–1883
28. Skovronsky, D. M., Moore, D. B., Milla, M. E., Doms, R. W., and Lee, V. M. (2000) *J. Biol. Chem.* **275,** 2568–2575
29. Zhou, Y., Suram, A., Venugopal, C., Prakasam, A., Lin, S., Su, Y., Li, B., Paul, S. M., and Sambamurti, K. (2008) *FASEB J.* **22,** 47–54
30. Kimberly, W. T., Zheng, J. B., Guenette, S. Y., and Selkoe, D. J. (2001) *J. Biol. Chem.* **276,** 40288–40292
31. Ni, Y., Zhao, X., Bao, G., Zou, L., Teng, L., Wang, Z., Song, M., Xiong, J., Bai, Y., and Pei, G. (2006) *Nat. Med.* **12,** 1390–1396
32. Liu, J., and Lin, A. (2005) *Cell Res.* **15,** 36–42
33. Vingtdeux, V., Hamdane, M., Gompel, M., Begard, S., Drobecq, H., Ghestem, A., Grosjean, M. E., Kostanjevecki, V., Grognet, P., Vanmechelen, E., Buee, L., Delacourte, A., and Sergeant, N. (2005) *Neurobiol. Dis.* **20,** 625–637
34. Lee, M. S., Kao, S. C., Lemere, C. A., Xia, W., Tseng, H. C., Zhou, Y., Neve, R., Ahlijanian, M. K., and Tsai, L. H. (2003) *J. Cell Biol.* **163,** 83–95
35. Ruffels, J., Griffin, M., and Dickenson, J. M. (2004) *Eur. J. Pharmacol.* **483,** 163–173
36. Zhu, X., Raina, A. K., Rottkamp, C. A., Aliev, G., Perry, G., Boux, H., and Smith, M. A. (2001) *J. Neurochem.* **76,** 435–441
37. Swatton, J. E., Sellers, L. A., Faull, R. L., Holland, A., Iritani, S., and Bahn, S. (2004) *Eur. J. Neurosci.* **19,** 2711–2719
38. Hartzell, H. C. (2007) *Science* **317,** 1331–1332

39. Beckman, K. B., and Ames, B. N. (1998) *Physiol. Rev.* **78,** 547–581
40. Babior, B. M., Kipnes, R. S., and Curnutte, J. T. (1973) *J. Clin. Investig.* **52,** 741–744
41. Li, J. M., Mullen, A. M., Yun, S., Wientjes, F., Brouns, G. Y., Thrasher, A. J., and Shah, A. M. (2002) *Circ. Res.* **90,** 143–150
42. Schallreuter, K. U., Moore, J., Wood, J. M., Beazley, W. D., Gaze, D. C., Tobin, D. J., Marshall, H. S., Panske, A., Panzig, E., and Hibberts, N. A. (1999) *J. Investig. Dermatol. Symp. Proc.* **4,** 91–96
43. Schallreuter, K. U., Moore, J., Wood, J. M., Beazley, W. D., Peters, E. M., Marles, L. K., Behrens-Williams, S. C., Dummer, R., Blau, N., and Thony, B. (2001) *J. Investig. Dermatol.* **116,** 167–174
44. Benzing, W. C., Wujek, J. R., Ward, E. K., Shaffer, D., Ashe, K. H., Younkin, S. G., and Brunden, K. R. (1999) *Neurobiol. Aging* **20,** 581–589
45. Liao, Y. F., Wang, B. J., Cheng, H. T., Kuo, L. H., and Wolfe, M. S. (2004) *J. Biol. Chem.* **279,** 49523–49532
46. Zhang, S., Lin, Y., Kim, Y. S., Hande, M. P., Liu, Z. G., and Shen, H. M. (2007) *Cell Death Differ.* **14,** 1001–1010
47. McLendon, C., Xin, T., Ziani-Cherif, C., Murphy, M. P., Findlay, K. A., Lewis, P. A., Pinnix, I., Sambamurti, K., Wang, R., Fauq, A., and Golde, T. E. (2000) *FASEB J.* **14,** 2383–2386
48. Jin, S. M., Cho, H. J., Jung, M. W., and Mook-Jung, I. (2007) *Cell Death Differ.* **14,** 189–192
49. Xie, Z., Dong, Y., Maeda, U., Moir, R. D., Xia, W., Culley, D. J., Crosby, G., and Tanzi, R. E. (2007) *J. Neurosci.* **27,** 1247–1254
50. Tamagno, E., Guglielmotto, M., Aragno, M., Borghi, R., Autelli, R., Giliberto, L., Muraca, G., Danni, O., Zhu, X., Smith, M. A., Perry, G., Jo, D. G., Mattson, M. P., and Tabaton, M. (2008) *J. Neurochem.* **104,** 683–695
51. Zhu, X., Raina, A. K., Perry, G., and Smith, M. A. (2004) *Lancet. Neurol.* **3,** 219–226